Journal of
Composites Science

MDPI

Article

Modification of Talc and Mechanical Properties of Polypropylene-Modified Talc Composite Drawn Fibers

Costas Tsioptsias [1,2,*], Konstantinos Leontiadis [2], Xanthi Ntampou [2] and Ioannis Tsivintzelis [2,*]

[1] Department of Chemical Engineering, University of Western Macedonia, 50132 Kozani, Greece
[2] Department of Chemical Engineering, Aristotle University of Thessaloniki, University Campus, 54124 Thessaloniki, Greece
* Correspondence: aff00285@uowm.gr (C.T.); tioannis@cheng.auth.gr (I.T.)

Abstract: A large amount of the polypropylene (PP) produced worldwide is used in the form of fibers. In this work, a new modification route for talc and PP is investigated, which is based on the in situ polymerization of a silane–siloxane monomer mixture on the surface of talc particles or PP pellets, respectively. The obtained modified talc and PP samples were used for the development of PP-talc composite drawn fibers. Tensile tests, thermogravimetry (TGA), and X-ray diffraction (XRD) were used for the characterization of the materials. It was observed that such a modification procedure resulted in the exfoliation of some talc particles. Enhanced tensile strength was observed for composite drawn fibers of a low talc content (1% with respect to PP) and a low modifier content (2% with respect to talc), while co-aggregation of talc and silicone may occur at high silicone and talc contents, resulting in the inferior mechanical performance of the corresponding composites. It was concluded that the produced silicone polymer simultaneously acts as a modifier, antioxidant, and compatibilizer. The proposed modification route is promising and should be further optimized.

Keywords: polypropylene; talc; nanocomposites; silicone; fiber; drawing

Citation: Tsioptsias, C.; Leontiadis, K.; Ntampou, X.; Tsivintzelis, I. Modification of Talc and Mechanical Properties of Polypropylene-Modified Talc Composite Drawn Fibers. *J. Compos. Sci.* **2024**, *8*, 91. https://doi.org/10.3390/jcs8030091

Academic Editors: Xiangfa Wu and Oksana Zholobko

Received: 20 January 2024
Revised: 22 February 2024
Accepted: 1 March 2024
Published: 3 March 2024

1. Introduction

PP is one of the most frequently used polymers. It exhibits numerous attractive properties such as low density, high thermal stability, and chemical inertness, and it allows for easy processing [1]. The inherent mechanical properties of PP, e.g., elastic modulus and tensile strength, are also high compared to those of various other polymers. Considerably enhanced tensile strength is exhibited by PP anisotropic-oriented structures that are produced by drawing (and the subsequent polymer chain orientation), which can be either uniaxial or biaxial [2]. Due to this enhancement, PP is widely used for the production of drawn sheets and fibers [3]. About 75% of the produced PP films are biaxially drawn, while almost 100% of the produced PP fibers are uniaxially drawn [2].

Melt spinning and solid-state stretching are the typical processes used for the production of drawn fibers. Although these are, in principle, rather simple processes, there are multiple factors that affect the structure and, consequently, the properties of the produced fibers. Among the factors that strongly influence fiber drawing are the molecular weight and the polydispersity of the polymer. The thermal behavior of the polymer (crystallization rate, glass transition, and crystallization temperatures) is also crucial for optimizing the properties of fibers [4].

The most common approach for improving the thermal and mechanical properties of polymers is via the use of additives and the development of composite materials. However, as mentioned in a recent review article [3], the improvement in the mechanical strength of drawn PP fibers or sheets due to the addition of fillers is much less than that achieved via the drawing process. The compatibility of the additive and the polymer matrix is considered to be of major importance for the enhancement of polymer's properties [5], e.g., for nylon [6],

poly(lactic acid) [7], and PP [8]. For this reason, there is a significant research interest for the modification and functionalization of additives, e.g., silane functionalization [9], or the modification of layered silicates [10] such as montmorillonite [11].

Very specialized PP modification is required in order to achieve compatibility with hydrophilic fillers, such as phyllosilicate minerals [12]. However, increased compatibility and exfoliation of the phyllosilicate mineral inside the polymer matrix may lead to increased crystallinity of the composite material [13], which is most often undesirable prior to drawing since it leads to inhomogeneous structures [4]. For example, in PP-modified montmorillonite drawn samples, the mineral acted as a nucleating agent and induced increased crystallinity of the composite materials, leading to the need to apply higher drawing temperatures [13]. In many cases, the composite PP fibers did not only not exhibit any significant improvement (compared to neat PP fibers) but rather showed a clear reduction in their mechanical strength, e.g., for PP–sepiolite [14], PP–hydrotalcite (perkalite), PP–montmorillonite [15], and PP–attapulgite [16]. For the case of attapulgite, such deterioration of the mechanical properties can be attributed to its known ability to act as a nucleating agent [17]. For this reason, attapulgite is commonly used as an additive only in non-drawn PP samples [18].

In other cases, it has been reported that the modified mineral did not act as a nucleating agent but rather as a processing additive, which resulted in increased drawing ability for the composite samples [19]. Similarly, for PP-POSS (polyhedral oligomeric silsesquioxane) composites, it has been reported that POSS acted as a "lubricating agent" that facilitates drawing [20]. Very often, common industrial additives, such as antioxidants, compatibilizers, dyes, and plasticizers, are firstly embedded in a polymer matrix of low molecular weight to facilitate mixing and adequate dispersion, forming a masterbatch that is subsequently mixed with the final polymer. It has been reported that such additives (antioxidant and compatibilizer) may significantly affect the drawing processing ability and the properties of drawn composite PP fibers through various ways, i.e., due to their lower molecular weight, or due to the existence of favorable intermolecular interactions between them that act competitively to those between the compatibilizer and the filler (e.g., talc and carbon nanotubes) [16].

The geometry of the filler is also quite important for the properties of the drawn composites. Needle-like fillers, such as carbon nanotubes, can align to the drawing axis due to mechanical stretching [21]. The alignment of particles and the polymer chains along the direction of stretching contributes to a symmetric stress transfer to the particles, which, in turn, decreases the accumulation of stress in certain regions (preventing the formation of early cracks). More precisely, upon exposure to mechanical stress, the molecules, atoms, particles, etc., of the material are forced to move. The movement of one region, e.g., an amorphous region, a crystal defect plane, etc., involves the transfer of stress to other regions. In aligned structures, the distribution of the applied stress is balanced (symmetric) throughout the material. In the case of random structures, the distribution of stress is random and not balanced and, thus, some regions are subjected to greater forces than other ones, leading to the formation of early cracks. Consequently, needle-like particles, such as carbon nanotubes [22–25] and wollastonite [16,26], have been widely used for the development of PP composite fibers. Also, it was shown that silica nanoparticles did not cause any significant improvement in the mechanical strength of a non-drawn polymer sample (tensile strength ~40 MPa); however, the tensile strength of the drawn sample (tensile strength ~196 MPa) was increased up to 270 MPa upon their addition. This was partially attributed to the spherical geometry of the nanoparticles and the formation of a percolated network, which enables stress transfer to amorphous regions [27].

Overall, as reported in a recent study, the established knowledge about polymer (nano-) composites (e.g., that an adequate dispersion of nanoparticles or an exfoliated structure of layered silicates results in improved mechanical properties) cannot be taken for granted for anisotropic structures due to the specificity of the drawing process and the specific structure of the drawn polymer matrices.

In this direction, in this work, we aim to explore the development of composite PP drawn fibers by minimizing the number of additives and, thus, reducing the number of possible negative interferences (e.g., by minimizing the content of low-molecular-weight additives in order to reduce any undesirable interactions between them). Talc was chosen since it is a common and cheap additive. Also, a silicon-based polymer was used for the modification of talc. Silicon-based materials can increase the thermal stability [28] and heat deflection temperature [29] of the polymer and can act as "lubricants" to facilitate drawing [20]. The silicon-based polymer contains Si-H groups, which are highly compatible with the C-H groups of PP and, thus, by modifying talc with such a polymer, the necessity of using an additional compatibilizer is avoided. Organosilanes have been grafted to clay and found to enhance the properties of the respective PP (non-drawn) composites [9]. Similar silicone-based materials have been used as coatings for the hydrophobicity enhancement of various substrates for outdoor applications and exhibit good adhesion [28,30]. Also, silicone is expected to enhance the thermal stability of PP, helping to avoid the use of additives, such as antioxidants or thermal stabilizers [28]. Next, we describe the modification route of talc and its influence on the tensile strength of PP composite drawn fibers.

2. Materials and Methods

2.1. Materials and Instruments

A masterbatch of neat isotactic PP (ECOLEN HZ42Q, Hellenic Petroleum S. A., Thessaloniki, Greece) with a Melt Flow Index of 18 g/10 min was used. Microtalc (Luzenac A3) with a median diameter of 1.1 μm was kindly provided by Imerys Minerals Ltd. (Paris, France). Nanotalc with an average particle size lower than 100 nm was obtained from Nanoshel LLC (Wilmington, DE, USA). A silane–siloxane mixture (SILRES BS290) was purchased from Wacker (Munich, Germany). Acetone (>99.5%) was purchased from Honeywell Riedel-de-Haen (Charlotte, North Carolina, USA).

A four-zone twin-screw extruder (Haake Rheodrive 5001, Thermo Fisher Scientific, Waltham, MA, USA), a three-zone single-screw extruder (Noztek Xcalibur, Shoreham-by-Sea, UK), a filament winder (Noztek, Shoreham-by-Sea, UK), and a homemade drawing apparatus were used for the preparation of the samples.

For the characterization of the samples, a Shimadzu TGA-50 (Shimadzu, Tokyo, Japan) Thermogravimetric analyzer (TGA) and a D8 Advance Bruker (Billerica, MA, USA) X-ray diffractometer (XRD) equipped with a Siemens X-ray source (Cu, 1.54 Å) were used. Tests for tensile strength were performed with a Hans Schmidt & Co GmbH Universal Testing Machine ZPM (Waldkraiburg, Germany) equipped with a Pacific load cell (model PA6110).

2.2. Talc and PP Modification

The silane–siloxane mixture was dissolved in acetone (2% w/v). In this solution, a certain amount of talc (or PP) was dispersed in order to achieve the desired silicone-to-talc (or PP) ratio. The mixture was constantly stirred until acetone was fully evaporated (stirring was possible up to some point). The samples were left at room temperature for 2 days. Such a period was chosen based on a separate experiment in which a solution of the silane–siloxane mixture was placed in a Petri dish at room conditions for 5 days. The film was macroscopically examined on a daily basis, and it was observed that after 2 days, solidification had occurred. Thus, it was deemed that a 2-day period is sufficient for the silicone-based polymer to be produced.

According to the adopted procedure, the silicone-based polymer is in situ produced on the surface of PP pellets or talc particles. Various modified talc and PP samples were prepared, as shown in Table 1.

Table 1. Names of the modified PP and talc samples and description.

Sample	Description
PP-2%sil	98% PP modified/coated with 2% silicone-based polymer
PP-3.3%sil	96.7% PP modified/coated with 3.3% silicone-based polymer
PP-10%sil	90% PP modified/coated with 10% silicone-based polymer
Microtalc-10%sil	90% microtalc and 10% silicone-based polymer
Nanotalc-10%sil	90% nanotalc and 10% silicone-based polymer
Nanotalc-2%sil	98% nanotalc and 2% silicone-based polymer
Nanotalc-sil-12 °C	Nanotalc sample obtained by vacuum filtering of a dispersion prepared at 12 °C
Nanotalc-sil-26 °C	Nanotalc sample obtained by vacuum filtering of a dispersion prepared at 26 °C

The PP-3.3%sil sample was used for some preliminary experiments in order to evaluate the thermal stability of the composites. In the case of talc, besides the adhesion on the surface, some molecules of the silane–siloxane mixture can be physically adsorbed in the interlayer space. In such a case, some intercalation may occur during polymerization. Of course, such a process is fundamentally different from the modification of other phyllosilicates, like montmorillonite, in which the modification is based on ion exchange. To check if adsorption occurs in the talc particles, the following experiment was carried out. Nanotalc was dispersed in a 5% w/v acetone solution of the silane–siloxane mixture. Two identical dispersions were prepared and were magnetically stirred for 5 h, with the only difference being temperature. One dispersion (nanotalc-sil-26 °C) was stirred at 26 °C (room temperature), while the other dispersion (nanotalc-sil-12 °C) was stirred at 12 °C. After stirring, the dispersions were vacuum filtered and left to dry in room conditions. These samples were examined with XRD (see Section 2.4 for more details). Adsorption is enthalpy-driven and is favored by the decrease in temperature. Thus, the talc sample that was treated at a lower temperature should exhibit the higher adsorption of silane–siloxane molecules and, thus, should present a more pronounced intercalated structure compared to the sample obtained at room temperature. It should be stressed that in this case (vacuum filtering), the actual talc-to-silane–siloxane mixture ratio is unknown.

2.3. Drawn Fiber Preparation

The neat and composite PP drawn fibers were prepared in three steps, namely, two extrusions and a solid-state drawing. The experimental apparatus and procedure have been described in detail in previous studies [16]. Briefly, the PP pellets and the talc powder were mechanically premixed inside a polyethylene bag by shaking. This mixture was then inserted in the twin-screw extruder (die of 3 mm, rotating speed of 25 rpm, temperature of the four zones: 190, 210, 215, 220 °C). The extruded filament was cooled in a water bath held at 12 ± 2 °C before being collected in the winder. This filament was pelletized and then inserted in the single screw extruder (die of 1.6 mm, rotating speed of 15 rpm, temperature of the three zones: 190, 210, 215 °C). Due to the lower die diameter of the second extruder, the extruded material was of lower diameter, and for this reason, instead of the term filament, we use the term fiber. Similarly to the extruded filament of the first extrusion, the extruded fiber of the second extrusion was cooled by immersion in a water bath held at 12 ± 2 °C and finally collected in the winder. The obtained fibers had a diameter of 0.4–0.7 mm. These fibers were subjected to solid-state drawing using an apparatus described in detail in previous studies [16]. Briefly, as shown in Figure 1, the fiber from the first winder is winded twice in the inlet low-diameter drum and is then inserted in an oven of constant temperature (140 ± 1 °C) through a small preheating zone (120 ± 2 °C). The filament is then winded twice in the outlet high-diameter drum and is finally driven in the second winder. The inlet and outlet drums rotate at the same speed, of 5 rpm. This way, the drawing ratio is equal to the ratio of their diameters (it was kept equal to 7 in all cases). The prepared drawn fiber samples are presented in Table 2.

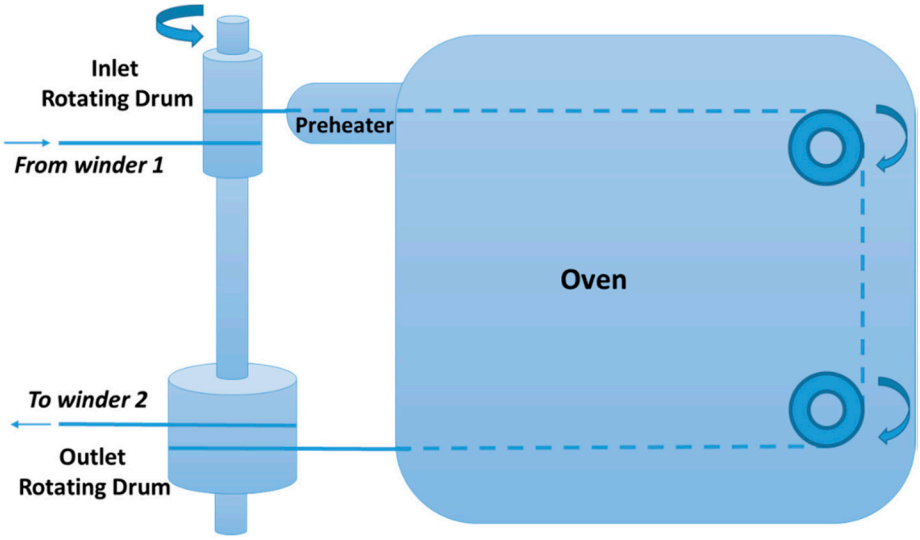

Figure 1. Scheme of the drawing apparatus.

Table 2. Names and description of the prepared drawn fiber samples.

	Sample	Description
1	PP	neat PP
2	PP-2%sil	PP modified with 2% silicone-based polymer
3	PP-10%sil	PP modified with 10% silicone-based polymer
4	PP-1.5% microtalc	neat PP with 1.5% unmodified microtalc
5	PP-1.5% microtalc-10%sil	neat PP with 1.5% microtalc modified with 10% silicone-based polymer
6	PP-1.5% nanotalc	neat PP with 1.5% unmodified nanotalc
7	PP-1.5% nanotalc-10%sil	neat PP with 1.5% nanotalc modified with 10% silicone-based polymer
8	PP-1% nanotalc-2%sil	neat PP with 1% nanotalc modified with 2% silicone-based polymer
9	PP-4% nanotalc-2%sil	neat PP with 4% nanotalc modified with 2% silicone-based polymer

2.4. Characterization

As mentioned in Section 2.1, the median diameter of the used microtalc particles was 1.1 μm, while the average diameter of the nanotalc particles was lower than 100 nm, as reported by the providers. The sample PP-3.3%sil, which was prepared during preliminary experiments, was studied by TGA in the 40 up to 450 °C temperature range at static air atmosphere and using a heating rate of 20 K/min. The neat nanotalc, the two modified nanotalc samples treated with 5% acetone solution and vacuum filtered (nanotalc-sil-12 °C and nanotalc-sil-26 °C), and the nanotalc-2%sil sample were examined with XRD using a step of 0.02° in the 5–90° range and a step of 0.01° in the 0–10° range. All the produced drawn fibers were characterized by tensile test measurements at room temperature using a head speed of 100 mm/min. For each sample, 8–12 independent measurements were carried out, and the results are presented as the average value (±standard deviation).

3. Results and Discussion

3.1. Talc Modification

In Figure 2a, the XRD graphs of neat and modified nanotalc are presented. The XRD graphs have been normalized to a scale from 0 to 1, and the graphs of the two modified samples (nanotalc-sil-12 °C and nanotalc-sil-26 °C) have been subtracted from the graph of pure nanotalc. This procedure, which is commonly used in FTIR spectroscopy [31], facilitates the direct observation of differences among the graphs. The subtracted graphs

are also presented in Figure 2a. The diffraction peaks of talc at 9.47°, 18.95°, and 28.64° are related to the interlayer space of talc corresponding, respectively, to the (002), (004), and (006) planes [32,33]. As can be seen in Figure 2a, the subtracted graph referring to the talc modified at 12 °C exhibits clear negative peaks at the abovementioned angles, indicating that the intensity of these peaks is reduced in the modified sample. In Figure 2b, suggestively, the negative peak at 9.47° and another peak at around 41°, which is clearly positive, are presented.

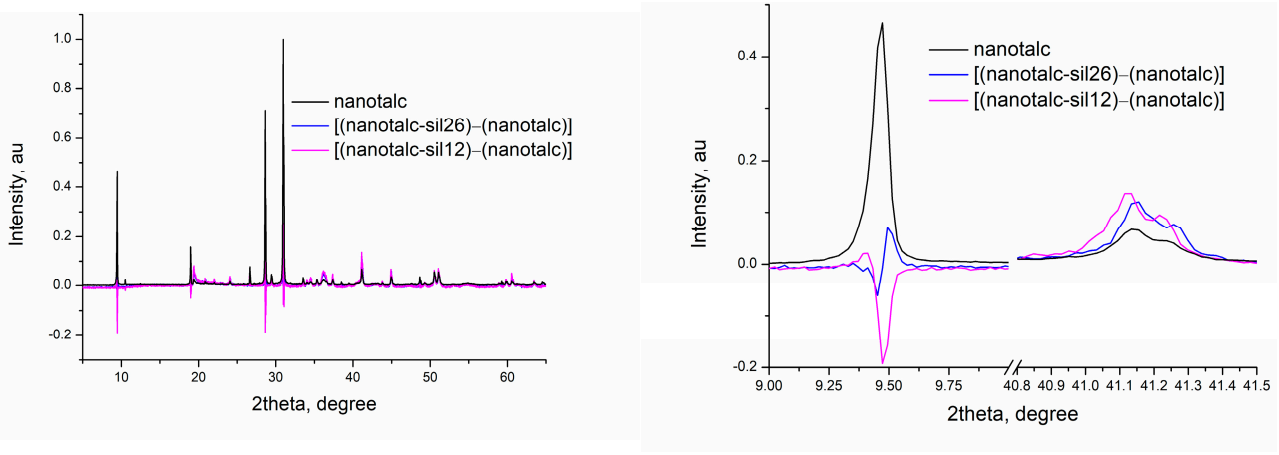

Figure 2. XRD of nanotalc and subtracted XRD graphs of the modified nanotalc samples prepared, respectively, at 26 °C [(nanotalc-sil-26 °C)–(nanotalc) subtracted graph] and 12 °C [(nanotalc-sil-12 °C)–(nanotalc) subtracted graph]: (**a**) in the range of 5–65°; (**b**) in the 9–9.75° and 40.8–41.5° ranges.

The relative decrease in these peaks indicates that some particles have been exfoliated. More precisely, it is true that the comparison of subtracted graphs is not common in XRD analysis, in contrast to FTIR analysis. However, both methods are volume-dependent (the intensity of a given peak of a substance is proportional to the volume fraction of this substance in the sample) and are used for quantitative analysis. The fact that only the peaks that are related to the interlayer distance of talc were found to be negative is a systematic and not a random change and points out that the volume fraction of these layers has decreased after modification. Perhaps, the only possibility for this to happen is partial exfoliation. A possible mechanism and explanation for this could be as follows. Initially, the majority of silane–siloxane molecules are adsorbed on the surface of all the talc particles and form a coating. Some monomer molecules are not adsorbed on the external surface but on the interspace layer. The reaction between the silane–siloxane molecules occurs spontaneously (upon exposure to moisture) and, thus, it is thermodynamically favored. Most likely, it is more favored than the adsorption on the talc surface or the interspace layer. Thus, as the polymerization reaction proceeds, the monomer molecules from the surface and from the interspace layer are desorbed and react with the already formed polymer and further increase its molecular weight. The desorption of these monomers is expected to have no influence on the interspace distance of talc particles. As in various other phenomena, it is known that the activation energy must be surpassed in order for the reaction to initiate. In interfaces, the energy barrier is often lower, and for this reason, it is likely that the polymerization reaction initiates at the interface of talc and monomer molecules and not in the bulk monomer mixture. Consequently, it is likely that the first oligomers are formed both on the surface and on the interlayer space of talc. Due to the increase in molecular weight during the polymerization reaction, the exfoliation of some talc particles is accomplished, while other particles remain intact. In the subtracted graph referring to the sample modified at 26 °C, no pronounced negative peaks are observed (see Figure 2b). This can be explained by the higher temperature that favors desorption, which is entropy-driven, and disfavors adsorption, which is enthalpy-driven.

As mentioned in the previous section, the actual composition of these raw modified talc samples is unknown due to the adopted procedure. These samples were not used for any PP composite preparation and were only prepared to investigate the modification of talc. In Figure 3, the XRD graph of the nanotalc-2%sil sample (98% nanotalc and 2% silicone-based polymer) is presented. Again, the graph is presented as a subtracted graph along with the graph of nanotalc.

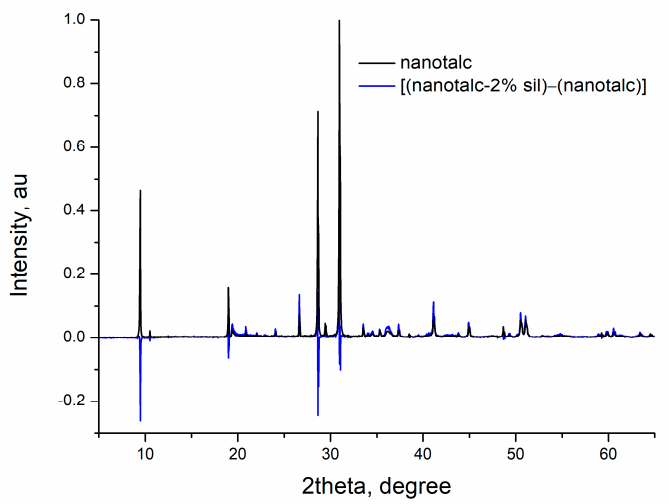

Figure 3. XRD of nanotalc and subtracted XRD graph of the nanotalc sample modified with 2% silicone-based polymer [(nanotalc 2%sil)–(nanotalc)].

It can be observed that this sample also exhibits negative peaks at angles related to the interlayer distance. Despite the fact that this modification was carried out at room temperature and not at a lower temperature, it seems that adsorption has occurred for the following reason. The procedure for the preparation of this sample was different from the procedure that was followed for the preparation of the other two samples, which are discussed in Figure 2. The abovementioned samples were removed from the solution of the silane–siloxane mixtures after 5 h of stirring and filtered, while the nanotalc-2%sil sample remained in the solution until complete evaporation of the solvent. Thus, the nanotalc-2%sil sample was exposed to a much higher amount of silane–siloxane mixture and, thus, it is reasonable to expect higher adsorption.

The above points out that such an in situ polymerization approach for the modification of talc is a very promising alternative for the modification of phyllosilicate minerals.

3.2. Preliminary Results on the Effect of Silicone-Based Polymer on Thermal Oxidation Stability of PP

In Figure 4, the TGA and derivative TGA curves of neat PP and PP-3.3%sil samples are presented. The typical application of this silicone polymer is hydrophobization. However, it has been reported that it contributes to the thermal oxidation stability and flame retardation of cellulose [28]. Thus, although in this work the main aim was to enhance the tensile strength of PP drawn fibers, it was checked whether the produced silicone can provide any thermal oxidation protection to PP as well. Indeed, as can be seen in Figure 4a, it seems that this is the case. The temperature of initiation of the thermal decomposition is more than 20 °C higher for the PP-3.3%sil sample compared to that of neat PP. From the derivative TGA curves (Figure 4b), it can be observed that the temperature of the maximum mass loss rate is approximately 350 °C for neat PP, while in the PP-3.3%sil sample, it is higher than 400 °C. Also, the maximum mass loss rate is lower for the modified sample. Clearly, the silicone-based polymer can act as a protecting agent for PP.

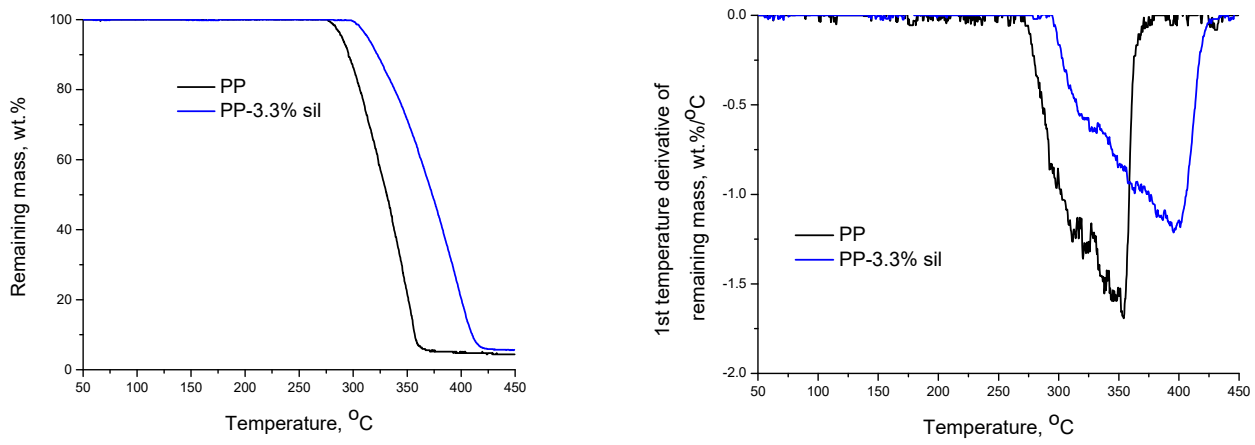

(**a**) (**b**)

Figure 4. (**a**) TGA curves of neat PP and PP-3.3%sil sample; (**b**) first temperature derivative TGA curves of neat PP and PP-3.3%sil drawn fibers.

In general, the thermal decomposition and thermal oxidation of polymers are complicated processes involving multiple phenomena. Thus, the recognition of the exact mechanism of the antioxidant activity of the silicone-based polymer requires a dedicated study. Here, we will briefly discuss some aspects that may explain the antioxidant activity of the silicone-based polymer. The C-C bond (that is the bond of the PP backbone) presents an average bond energy (or bond strength or dissociation energy) of 347 kJ/mol [34], while the average bond energy of Si-O (that is the backbone bond of siloxane polymers) is quite a bit higher and equal to 452 kJ/mol [34]. The values of other bonds of these two polymers are pretty similar, e.g., the average bond energies of C-H and Si-H are 413 and 393 kJ/mol, respectively [34]. Thus, in the presence of the silicone polymer, there is an increased number of strong bonds per unit mass of the (composite) material. Stronger bonds are less easily attacked by heat, oxygen, etc., and lead to better thermal stability. In addition, it is known [35] that at the early stage of polymer degradation through random scission, some of the decomposition products are too large to vaporize. Similarly, thermal oxidation is also accompanied by scission reactions, and some of the products may present rather high molecular weight, while reactions between such silicone polymer and the PP residues are possible. Some of the produced bonds may be stronger than the C-C bonds, e.g., the Si-C bond has an average bond energy of 360 kJ/mol, which is slightly higher than the one of C-C (347 kJ/mol) [34]. This could explain the increasing difference between the mass loss profiles of neat and modified PP as temperature increases, as well as the lower maximum mass loss rate and the higher temperature at which maximum mass loss occurs that were observed for the modified PP sample.

3.3. Mechanical Properties of PP Composite Drawn Fibers

3.3.1. Effect of Silicone on the Mechanical Properties of PP Drawn Fibers

In Table 3, the results of the tensile tests for the neat PP and composite PP drawn fibers are presented. Firstly, we will discuss the results that refer to samples 1, 2, and 3 in order to examine the influence of the silicone-based polymer on the tensile strength of the PP composite drawn fibers. In general, the addition of a rubbery polymer, such as silicone, in the PP matrix is expected to reduce the tensile strength and the elastic modulus of the composite material and to increase the elongation at break. However, as revealed in the previous section (see the TGA results), silicone acts as an antioxidant protecting the thermal decomposition of PP during fiber processing (two extrusions and one high-temperature solid-state drawing), and such behavior tends towards better mechanical properties for the composite material. Consequently, the addition of the silicone polymer has a dual effect on the mechanical properties of the composite fibers. As revealed by the results of Table 3,

upon the addition of 2% silicone, the latter phenomenon prevails, and the tensile strength seems to be marginally increased (see results for samples 1 and 2). However, upon the addition of 10%, the expected behavior is observed, i.e., sample 3 presents decreased tensile strength compared to sample 1.

Table 3. Results of the tensile tests for the neat PP and PP composite drawn fibers.

	Sample	Elastic Modulus, MPa	Stress at Break, MPa	Elongation at Break
1	Neat PP	2138 ± 186	360 ± 57	77 ± 7
2	PP-2%sil	2179 ± 283	383 ± 16	62 ± 3
3	PP-10%sil	1789 ± 242	331 ± 56	104 ± 6
4	PP-1.5% microtalc	2349 ± 288	356 ± 47	79 ± 4
5	PP-1.5% microtalc-10%sil	2805 ± 387	390 ± 47	72 ± 6
6	PP-1.5% nanotalc	2515 ± 342	366 ± 18	70 ± 4
7	PP-1.5% nanotalc-10%sil	2076 ± 512	340 ± 40	67 ± 4
8	PP-1% nanotalc-2%sil	2445 ± 581	421 ± 62	56 ± 4
9	PP-4% nanotalc-2%sil	1615 ± 338	343 ± 47	83 ± 7

3.3.2. Effect of Talc Modification on the Mechanical Properties of PP Composite Drawn Fibers

The comparison of samples 1 and 4 (see Table 3) reveals that the addition of 1.5% unmodified microtalc results in the typical behavior of micro-composites, i.e., a small increase in the elastic modulus and a (small here) deterioration of tensile strength. However, sample 5, which has been prepared with modified talc, exhibits both higher modulus and stress at break than both samples 1 and 4. This could be attributed to two factors: (a) the beneficial antioxidant activity of silicone (as revealed by the TGA measurements), and (b) the exfoliation of some talc particles (as revealed by the XRD measurements).

By comparing samples 1, 6, and 7, the respective discussion for nanotalc, as above for microtalc, can be carried out. The addition of 1.5% unmodified nanotalc seems to increase the elastic modulus and to have a small influence on tensile strength. The addition of modified nanotalc (with 10% silicone-based polymer, sample 7) seems to cause a deterioration of tensile strength. Having in mind the results for the PP composite with 1.5% modified microtalc (sample 4), this behavior of the modified nanotalc was unexpected, since nanocomposites are, in general, expected to perform better than microcomposites. Perhaps this behavior is caused by the high amount of the modifier (10%), which interferes with the process in various ways. In more detail, such a negative effect may be attributed to the poor mechanical strength of the silicone-based polymer, as well as its low molecular weight (compared to that of PP). Such low molecular weight imposes a limitation to the drawing process, since it is known that the overstretching of short polymer chains results in the deterioration of the final mechanical properties [3]. In addition, this problem could be intensified by the high polydispersity of the silicone polymer, which is expected due to the uncontrolled polymerization of the silane–siloxane mixture, e.g., the temperature of the reaction is not controlled.

In order to further investigate the latter point, two new PP-nanotalc composite drawn fiber samples were prepared, but with a lower content of the modifier (2%), one containing 1% nanotalc (sample 8) and one containing 4% nanotalc (sample 9). Sample 8 (PP-1%nanotalc-2%sil) clearly appears to be superior to all of the investigated samples and exhibits, by far, the highest tensile strength. The deterioration of the properties at high nanotalc contents (4% for sample 9) can be considered as the typical behavior of nanocomposites, i.e., only a rather very small amount of the filler increases the mechanical strength. Considering sample 8 (PP-1%nanotalc-2%sil), it seems that the increased stability of PP over thermal oxidation (supported by TGA) and the partial exfoliation of talc (supported by XRD) due to the presence of the silicone-based polymer overcompensate any of the negative effects discussed above.

4. Further Discussion

As discussed in the Introduction section, a considerable increase in tensile strength is achieved by drawing, which is incomparably higher than any increase accomplished by the addition of fillers. This is the case also for the results of this study. The non-drawn neat PP sample exhibits a tensile strength of around 35 MPa, which was increased up to 360 MPa simply by drawing (930% increase in tensile strength). For the PP composite sample that performed better (sample 8, PP-1%nanotalc-2%sil), the addition of the modified filler further increased the tensile strength from 360 to 420 MPa, which corresponds to an additional increase of 17%.

Such an improvement is low, but it is not negligible. It is higher than the corresponding one shown by other PP–composite drawn fibers that were investigated in our previous studies and were prepared by the very same procedure (two extrusions, drawing with the same ratio and drawing temperature and using the same equipment) [16]. In more detail, in our previous works, we prepared PP composite drawn fibers with various fillers, such as wollastonite, attapulgite, carbon nanotubes, montmorillonite, microtalc, and ultrafine talc, using a drawing ratio of seven, and various important additives, such as an antioxidant and PP grafted with maleic anhydrite as a compatibilizer. However, we rarely observed a value of tensile strength higher than 400 MPa. Thus, though an increase of 17% seems low, it is promising if it is taken into account that, besides the filler, only one additive (the silicone polymer), which has multiple effects as it acts as both a talc modifier, polymer compatibilizer, and antioxidant, was used in this approach.

Thus, besides the direct action of the modified talc, it is possible that there was an indirect contribution to the improvement in mechanical properties which originates from the fact that the use of low-molecular-weight additives was minimized. Consequently, the proposed modification route for talc seems to be promising and should be further studied and optimized.

Optimization is necessary, especially for the modification approach of talc and PP. As it was shown, a high content of the silicone polymer causes deterioration of the mechanical strength of the PP fibers in the absence of talc, but lower contents appeared to be beneficial. A fine tuning of this amount should be performed. However, such optimization should be simultaneously performed both for talc and PP and not only for PP, since the optimum amount of silicone for neat PP may not be the optimum in the case of PP-modified talc composites. For studying the effect of multiple independent variables on response variables (e.g., tensile strength), the design of the experiments based on the surface response analysis is a very attractive option. Additionally, the major drawback of the second approach, which was used for the modification of talc, is high uncertainty regarding the amount of silicone polymer that is added to talc. Of course, careful filtering and accurate weighting before and after modification could solve this problem. Though talc modified by this approach was not used for producing PP composite fibers, this approach may have the following advantage. In the talc sample, which is produced by the first approach, a large amount of the monomer mixture is on the surface of talc particles, forming a coating, and only a very small amount is likely to be adsorbed on the interspace layers. The high silicone content on the surface of talc may contribute to the deterioration of the mechanical properties, and this would be more intense if PP was also treated with silicone. On the contrary, in the talc was modified with the second approach, the amount of silicone on the surface of the talc particles is expected to be less, and this may minimize any negative effects. In both approaches for the modification of talc, the use of organic solvent is necessary, and this is a drawback related to environmental and health issues as well as cost issues. In a potential application on an industrial scale, the volatility and flammability of acetone will also raise safety issues. Finally, the modification process is a rather time-consuming process, and additional costs would be required in order to accelerate it, e.g., to include a drying stage. Of course, such issues are also present in other modification processes, e.g., the modification of montmorillonite, which occurs is aqueous solution.

5. Conclusions

A novel route for the modification of phyllosilicate minerals, and particularly talc, was explored. The modification was based on the adsorption of silane–siloxane monomer mixture on talc particles and the in situ synthesis of a silicone polymer. During the polymerization of the silane–siloxane mixture and the corresponding increase in molecular weight, some talc particles were exfoliated, as concluded by XRD measurements. On top of that, it was observed that the introduction of the obtained silicone polymer inside the PP matrix increases the thermal stability of the composite material. Consequently, the produced silicone polymer simultaneously acts as a talc modifier, as an antioxidant, and as a polymer compatibilizer. The introduction of silicone polymer inside the PP matrix at high contents deteriorates the tensile strength of PP drawn fibers. Also, the co-aggregation of talc and silicone may occur at high silicone contents, resulting in the inferior mechanical performance of the corresponding composites. However, at a low talc content (1% with respect to PP) and a low modifier content (2% with respect to talc), very promising results were obtained, and the average value of the stress at break increased by 17% (from 360 to 421 MPa). The optimization of the talc's modification route might result in a further enhancement of the tensile strength of PP drawn fibers.

Author Contributions: Conceptualization, C.T. and I.T.; methodology, C.T.; software, C.T. and K.L.; validation, C.T., K.L. and I.T.; formal analysis, C.T., K.L. and I.T.; investigation, C.T., X.N. and K.L.; resources, I.T.; writing—original draft preparation, C.T.; writing—review and editing, K.L. and I.T.; supervision, I.T.; project administration, I.T. All authors have read and agreed to the published version of the manuscript.

Funding: The authors gratefully acknowledge financial support by the European Regional Development Fund of the European Union and Greek national funds through the Operational Program Competitiveness, Entrepreneurship, and Innovation, under the call INDUSTRIAL MATERIALS (project code: T6YBP-00035).

Data Availability Statement: Data available upon request.

Conflicts of Interest: The authors declare no conflicts of interest.

References

1. Galli, P.; Danesi, S.; Simonazzi, T. Polypropylene based polymer blends: Fields of application and new trends. *Polym. Eng. Sci.* **1984**, *24*, 544–554. [CrossRef]
2. Moore, E.P. (Ed.) *Polypropylene Handbook: Polymerization, Characterization, Properties, Processing, Applications*; Hanser Publishers: Liberty Twp, OH, USA, 1996.
3. Tsioptsias, C.; Leontiadis, K.; Tzimpilis, E.; Tsivintzelis, I. Polypropylene nanocomposite fibers: A review of current trends and new developments. *J. Plast. Film Sheeting* **2021**, *37*, 283–311. [CrossRef]
4. Eichhorn, S.; Hearle, J.W.S.; Jaffe, M.; Kikutani, T. *Handbook of Textile Fibre Structure: Volume 1: Fundamentals and Manufactured Polymer Fibres*; Elsevier Science: Amsterdam, The Netherlands, 2009.
5. Okada, A.; Usuki, A. The chemistry of polymer-clay hybrids. *Mater. Sci. Eng. C* **1995**, *3*, 109–115. [CrossRef]
6. Cho, J.W.; Paul, D.R. Nylon 6 nanocomposites by melt compounding. *Polymer* **2001**, *42*, 1083–1094. [CrossRef]
7. Marras, S.I.; Zuburtikudis, I.; Panayiotou, C. Nanostructure vs. microstructure: Morphological and thermomechanical characterization of poly(l-lactic acid)/layered silicate hybrids. *Eur. Polym. J.* **2007**, *43*, 2191–2206. [CrossRef]
8. Cimmino, S.; Duraccio, D.; Silvestre, C.; Pezzuto, M. Isotactic polypropylene modified with clay and hydrocarbon resin: Compatibility, structure and morphology in dependence on crystallization conditions. *Appl. Surf. Sci.* **2009**, *256*, S40–S45. [CrossRef]
9. Raji, M.; Mekhzoum, M.E.M.; Rodrigue, D.; Qaiss, A.e.k.; Bouhfid, R. Effect of silane functionalization on properties of polypropylene/clay nanocomposites. *Compos. Part B Eng.* **2018**, *146*, 106–115. [CrossRef]
10. Vaia, R.A.; Giannelis, E.P. Lattice Model of Polymer Melt Intercalation in Organically-Modified Layered Silicates. *Macromolecules* **1997**, *30*, 7990–7999. [CrossRef]
11. Yuan, Y.; Yu, B.; Wang, W. The influence of poorly-/well-dispersed organo-montmorillonite on interfacial compatibility, fire retardancy and smoke suppression of polypropylene/intumescent flame retardant composite system. *J. Colloid Interface Sci.* **2022**, *622*, 367–377. [CrossRef] [PubMed]
12. Manias, E.; Touny, A.; Wu, L.; Strawhecker, K.; Lu, B.; Chung, T.C. Polypropylene/Montmorillonite Nanocomposites. Review of the Synthetic Routes and Materials Properties. *Chem. Mater.* **2001**, *13*, 3516–3523. [CrossRef]

13. Joshi, M.; Shaw, M.; Butola, B.S. Studies on composite filaments from nanoclay reinforced polypropylene. *Fibers Polym.* **2004**, *5*, 59–67. [CrossRef]
14. Vargas, A.F.; Orozco, V.H.; Rault, F.; Giraud, S.; Devaux, E.; López, B.L. Influence of fiber-like nanofillers on the rheological, mechanical, thermal and fire properties of polypropylene: An application to multifilament yarn. *Compos. Part A Appl. Sci. Manuf.* **2010**, *41*, 1797–1806. [CrossRef]
15. Lorenzi, D.; Sartori, G.; Ferrara, G.; Fambri, L. Spinnability of Nanofilled Polypropylene. *Macromol. Symp.* **2011**, *301*, 73–81. [CrossRef]
16. Tsioptsias, C.; Leontiadis, K.; Messaritakis, S.; Terzaki, A.; Xidas, P.; Mystikos, K.; Tzimpilis, E.; Tsivintzelis, I. Experimental Investigation of Polypropylene Composite Drawn Fibers with Talc, Wollastonite, Attapulgite and Single-Wall Carbon Nanotubes. *Polymers* **2022**, *14*, 260. [CrossRef]
17. Medeiros, E.S.; Tocchetto, R.S.; Carvalho, L.H.; Conceição, M.M.; Souza, A.G. Nucleating Effect and Dynamic Crystallization of a Poly(propylene)/Attapulgite System. *J. Therm. Anal. Calorim.* **2002**, *67*, 279–285. [CrossRef]
18. Xia, Y.; Zhu, Y.; Zhou, Y.; Nie, W.; Chen, P. Improved dispersion of attapulgite in polypropylene by grap oxide and the enhanced mechanical properties. *Polym. Compos.* **2018**, *39*, 560–568. [CrossRef]
19. van Erp, T.B.; Reynolds, C.T.; Bilotti, E.; Peijs, T. Nanoclay assisted ultra-drawing of polypropylene tapes. *Nanocomposites* **2019**, *5*, 114–123. [CrossRef]
20. Butola, B.S.; Joshi, M.; Kumar, S. Hybrid organic-inorganic POSS (polyhedral oligomeric silsesquioxane)/polypropylene nanocomposite filaments. *Fibers Polym.* **2010**, *11*, 1137–1145. [CrossRef]
21. Jin, L.; Bower, C.; Zhou, O. Alignment of carbon nanotubes in a polymer matrix by mechanical stretching. *Appl. Phys. Lett.* **1998**, *73*, 1197–1199. [CrossRef]
22. McIntosh, D.; Khabashesku, V.N.; Barrera, E.V. Nanocomposite Fiber Systems Processed from Fluorinated Single-Walled Carbon Nanotubes and a Polypropylene Matrix. *Chem. Mater.* **2006**, *18*, 4561–4569. [CrossRef]
23. Dondero, W.E.; Gorga, R.E. Morphological and mechanical properties of carbon nanotube/polymer composites via melt compounding. *J. Polym. Sci. Part B Polym. Phys.* **2006**, *44*, 864–878. [CrossRef]
24. Acierno, S.; Barretta, R.; Luciano, R.; Marotti de Sciarra, F.; Russo, P. Experimental evaluations and modeling of the tensile behavior of polypropylene/single-walled carbon nanotubes fibers. *Compos. Struct.* **2017**, *174*, 12–18. [CrossRef]
25. Deng, H.; Bilotti, E.; Zhang, R.; Peijs, T. Effective reinforcement of carbon nanotubes in polypropylene matrices. *J. Appl. Polym. Sci.* **2010**, *118*, 30–41. [CrossRef]
26. Leontiadis, K.; Achilias, D.S.; Tsivintzelis, I. Effect of the Filler Modification on the Thermal and Mechanical Properties of Composite Polypropylene/Wollastonite Drawn Fibers. *Polymers* **2023**, *15*, 2986. [CrossRef] [PubMed]
27. Wang, M.H.; Ruan, W.H.; Huang, Y.F.; Ye, L.; Rong, M.Z.; Zhang, M.Q. A strategy for significant improvement of strength of semi-crystalline polymers with the aid of nanoparticles. *J. Mater. Chem.* **2012**, *22*, 4592–4598. [CrossRef]
28. Kivotidi, S.; Tsioptsias, C.; Pavlidou, E.; Panayiotou, C. Flame-retarded hydrophobic cellulose through impregnation with aqueous solutions and supercritical CO2. *J. Therm. Anal. Calorim.* **2013**, *111*, 475–482. [CrossRef]
29. Singh, U.P.; Biswas, B.K.; Ray, B.C. Evaluation of mechanical properties of polypropylene filled with wollastonite and silicon rubber. *Mater. Sci. Eng. A* **2009**, *501*, 94–98. [CrossRef]
30. Manoudis, P.N.; Karapanagiotis, I.; Tsakalof, A.; Zuburtikudis, I.; Panayiotou, C. Superhydrophobic Composite Films Produced on Various Substrates. *Langmuir* **2008**, *24*, 11225–11232. [CrossRef]
31. Stuart, B. *Infrared Spectroscopy: Fundamentals and Applications*; John Wiley and Sons Ltd.: West Sussex, UK, 2004.
32. Shao, W.; Wang, Q.; Li, K. Intercalation and exfoliation of talc by solid-state shear compounding (S3C) using pan-mill equipment. *Polym. Eng. Sci.* **2005**, *45*, 451–457. [CrossRef]
33. Huang, X.; Li, J.; Su, X.; Fang, K.; Wang, Z.; Liu, L.; Wang, H.; Yang, C.; Wang, X. Remarkable damage in talc caused by electron beam irradiation with a dose of up to 1000 kGy: Lattice shrinkage in the Z- and Y-axis and corresponding intrinsic microstructural transformation process speculation. *RSC Adv.* **2021**, *11*, 21870–21884. [CrossRef]
34. Zumdahl, S.S.; Zumdahl, S.A.; DeCoste, D.J. *Chemistry*; Cengage Learning: Boston, MA, USA, 2018.
35. Flynn, J.H.; Wall, L.A. General Treatment of the Thermogravimetry of Polymers. *J. Res. Natl. Bur. Stand. A Phys. Chem.* **1966**, *70A*, 487–523. [CrossRef] [PubMed]